High-throughput screening of the ReFRAME library identifies potential drug repurposing candidates for *Trypanosoma cruzi*

Jean A. Bernatchez[a,b], Emily Chen[c], Mitchell V. Hull[c], Case W. McNamara[c], James H. McKerrow[a,b], Jair L. Siqueira-Neto[a,b]#

Running Title: Drug repurposing for *T. cruzi*

[a]Skaggs School of Pharmacy and Pharmaceutical Sciences, University of California, San Diego, La Jolla, California, USA

[b]Center for Discovery and Innovation in Parasitic Diseases, University of California, San Diego, La Jolla, California, USA

[c]Calibr, a division of The Scripps Research Institute, La Jolla, California, USA

#Address correspondence to Jair Siqueira-Neto, jairlage@health.ucsd.edu

Abstract

Chagas disease, caused by the kinetoplastid parasite *Trypanosoma cruzi*, affects between 6 and 7 million people worldwide, with an estimated 300,000 to 1 million of these cases in the United States. In the chronic phase of infection, *T. cruzi* can cause severe gastrointestinal and cardiac disease, which can be fatal. Currently, only benznidazole is clinically-approved by the FDA for pediatric use to treat this infection in the USA. Toxicity associated with this compound has driven the search for new anti-Chagas agents. Drug repurposing is a particularly attractive strategy for neglected diseases, as pharmacological parameters and toxicity are already known for these compounds, reducing costs and saving time in the drug development pipeline. Here, we screened ~ 12,000 compounds from the ReFRAME library, a collection of drugs or compounds with confirmed clinical safety, against *T. cruzi*. We identified 7 compounds of interest with potent *in vitro* activity against the parasite with a therapeutic index of 10 or greater, including the previously-unreported activity of the antiherpetic compound 348U87. These results provide the framework for further development of new *T. cruzi* leads that can potentially move quickly to the clinic.

Keywords: *Trypanosoma cruzi*, antiparasitics, high-throughput screening, drug repurposing

Introduction

Trypanosoma cruzi, the causative agent of Chagas disease, is a protozoan parasite that is primarily transmitted to humans via triatomine insects (known as kissing bugs) during a blood meal. Infection by *T. cruzi* manifests initially in an acute phase of infection, and if left untreated, proceeds to a chronic phase (1). During the acute phase, mild or unremarkable symptoms such as fever, fatigue, rash, headache or swelling at the site of the triatome bite may present. When left untreated, the primary infection usually resolves in weeks, but residual parasites remain in the host's body evolving to the chronic phase. Over the span of years to decades, approximately 30% of those infected individuals will manifest cardiac and/or gastrointestinal complications leading to morbidity and mortality (2).

Current treatment options are very limited for Chagas disease: only benznidazole is clinically-approved for pediatric use in the case of acute *T. cruzi* infections in the United States. Benznidazole and nifurtimox are available off-label via the CDC for compassionate use for all other cases of this infection. However, severe side-effects associated with the use of these medications leads to high levels of patient discontinuation of treatment. Furthermore, the usefulness of benznidazole in the chronic phase of infection is disputed within the Chagas research community (3–5).

Limited efforts from the pharmaceutical industry to develop a medication for *T. cruzi* infections further complicates progress towards anti-Chagas agents better than benznidazole and nifurtimox. Rising costs and high levels of failure of drug molecules in clinical trials due to adverse events and lack of efficacy present further general barriers to the development of medications. One cost-effective strategy involves repurposing

existing drugs with known toxicity and pharmacokinetic profiles for other indications (6). This has the potential to speed up drug development efforts, reduce costs and lower the chance of adverse events presenting in clinical trials. The ReFRAME (Repurposing, Focused Rescue, and Accelerated Medchem) library, a comprehensive set of molecules with tested clinical safety, has been previously used to identify potential drug repurposing hits for neglected tropical diseases (7, 8). In this work, we screened 7,680 compounds from this library against the medically relevant intracellular, amastigote form of *T. cruzi* infecting mouse myoblasts using a high-throughput, phenotypic cellular imaging assay that our group has successfully used in previous studies to identify novel antitrypanosomal agents (9–11). We identified seven compounds with suitable selectivity indexes (SIs) for drug repurposing; two of these, the antiherpetic drug 348U87 and the serotonin receptor binder 3-[4-[4-(2-Methoxyphenyl)piperazine-1-yl]butyl]-6-[2-[4-(4-fluorobenzoyl)piperidine-1-yl]ethyl]benzothiazole-2(3H)-one, have not previously been reported as anti-Chagas compounds and may target the parasite through a novel mechanism. These molecules form an attractive collection of lead molecules for potential drug repurposing to treat Chagas disease.

Results

Primary screening of the ReFRAME library against T. cruzi *using a high-content imaging assay.*

Compounds from the ReFRAME library were pre-spotted on 1536 clear-bottom black well plates in 100% dimethylsulfoxide (DMSO) for a final concentration of 10 µM in 10 µL final volume (and 0.1% DMSO final concentration). C212 mouse myoblasts and

CA-I/72 strain *T. cruzi* trypomastigotes were added to the plate in a 15:1 infection ratio and incubated for 72 hours at 37°C and 5% CO_2. Cells were then fixed with 4% paraformaldehyde (final concentration), and stained with 5 µg/ml of 4',6-diamidino-2-phenylindole (DAPI) to highlight the nuclei from the host cells and parasites. Using an ImageXpress MicroXL automated microscope (10x magnification setting), fluorescence images of C2C12 and *T. cruzi* amastigote nuclei were acquired for each well, and the number of host cell nuclei and amastigote nuclei were automatically determined using a custom image analysis module as previously described (9–11) (Figure 1). Infection levels were calculated as a ratio of the number of *T. cruzi* amastigotes per C2C12 host cell as determined by nuclei counting. Compound toxicity was determined by dividing the number of host cell nuclei in a drug-treated well to the average of the vehicle controls. For both infection ratios and cell viability ratios, values were normalized to the vehicle controls to determined percent activity and toxicity, respectively. Control wells containing uninfected C2C12 cells, infected C2C12 cells with 0.1% DMSO, and infected C2C12 cells with 0.1% DMSO and 50 µM benznidazole were prepared in each plate for data normalization. The mean Z' for the 10 plates tested was 0.52 with a standard error of 0.01. Hit selection cutoffs for the primary screen were set at 70% antiparasitic activity (70% parasite reduction compared to untreated controls) and 50% host cell viability at 10 µM compound compared to untreated controls (represents approximately 3 standard deviations from the average of the untreated controls). We identified 238 compounds (2% of the total library) that met these selection criteria. A summary of the primary screening data is shown in Figure 2.

Counter-screen of 238 hits in dose response

To validate the hits obtained from our primary screen, compounds were re-spotted in duplicate in a 10-point, 3-fold dilution dose response, with 10 µM as the highest concentration of inhibitor. Using the high-content imaging assay, 238 primary hits were retested in duplicate. We identified seven compounds of interest using the following cutoff criteria: at least 70% antiparasitic activity at a given drug concentration in one of the two dose response replicates and a therapeutic index of 10 or greater. Half maximal effective concentration (EC_{50}), half maximal cytotoxic concentration (CC_{50}) and selective index (SI; defined by the ratio of CC_{50} to EC_{50}) for validated hits are shown in Table 1, their dose response curves are shown in Figure 3 and the chemical structures of these compounds are displayed in Figure 4. The 7 compounds retained were NSC-706744, 348U87, ASP-8273, XR 5944, Prenyl-IN-1, 3-[4-[4-(2-Methoxyphenyl)piperazine-1-yl]butyl]-6-[2-[4-(4-fluorobenzoyl)piperidine-1-yl]ethyl]benzothiazole-2(3H)-one and incadronate disodium.

Discussion

Given the toxicity of currently available drugs to treat *T. cruzi* infection, research efforts have been made to explore additional candidate molecules against the parasite. In this work, we screened a drug repurposing library for compounds with anti-Chagasic activity. We identified 7 molecules as having potent *in vitro* activity against *T. cruzi* and a SI of at least 10 against C2C12 cardiomyocyte host cells.

As validation for our assay, we identified a number of compounds from classes which have previously been reported as having anti-Chagas activity, namely

farnesyltransferase inhibitors (12–16) (Prenyl-IN-1, incadronate disodium) and DNA topoisomerase inhibitors (17–20) (NSC-706744, XR 5944).

We also identified the EGFR inhibitor ASP-8273 (naquotinib) (21–23) as an inhibitor of *T. cruzi* with good potency (EC_{50} of 2.7 nM) and a SI of 191. Several studies have successfully explored kinase inhibitors of trypanosomatids as therapeutic agents (24–26), and this compound may represent yet another possible candidate for repurposing or further chemical derivatization.

Interestingly, we identified two compounds with intriguing primary indications that may target *T. cruzi* by novel mechanisms. First, serotonin receptor ligands such as 3-[4-[4-(2-Methoxyphenyl)piperazine-1-yl]butyl]-6-[2-[4-(4-fluorobenzoyl)piperidine-1-yl]ethyl]benzothiazole-2(3H)-one (27) have been investigated as agents to treat anxiety and panic disorders. This compound had an EC_{50} of 22 nM and a SI of 145, making it an attractive candidate for drug repurposing and animal model testing. Second, the herpes virus drug 348U87 (EC_{50} of 0.63 nM and a SI of 1294), which targets the viral ribonucleotide reductase (28–31), has been shown to potentiate the activity of acyclovir in topical applications. The thiosemicarbazone iron chelator 3-AP has also been shown to inactivate the ribonucleotide reductase of *T. brucei* (32), and 348U87 may act against a homologous protein of *T. cruzi* in a similar manner. For both of the afore-mentioned compounds, mechanistic studies are planned and ongoing to identify the precise molecular targets of these inhibitors.

Follow-up studies in our group will test our most promising compounds in mouse models of *T. cruzi* infection to establish proper dosing protocols and *in vivo* efficacy. In sum, these compounds represent new potent new leads with known pharmacological

parameters and possibly novel mechanisms of action against *T. cruzi*, making them attractive candidates for accelerated development as anti-Chagas agents.

Materials and Methods

Cells.

C2C12 mouse myoblasts (ATCC CRL-1772) and CA-I/72 *T. cruzi* (kindly donated by J. Dvorak, NIH) were cultured in Dubelco's Modified Eagle Medium (Invitrogen, 11095-080) supplemented with 5% fetal bovine serum (Sigma Aldrich, F2442) and 1% penicillin-streptomycin (Invitrogen, 15140122) at 37°C and 5% CO_2 essentially as described (11). Passaging of CA-I/72 *T. cruzi* was conducted weekly via co-culture with C2C12 host cells.

Phenotypic imaging assay.

Compounds from ReFRAME library, benznidazole (Sigma cat. no. 419656) and DMSO (Sigma cat. no. D2650) were transferred to black 1536-well plates (Greiner Bio One, 782092) with clear bottoms using an Acoustic Transfer System (ATS) instrument (EDC Biosystems). C2C12 cells were seeded at a density of 100 cells per well and CA-I/72 *T. cruzi* parasites were seeded at a density of 1,500 cells per well using a Multidrop Combi liquid handler (Thermo Scientific). Plates were incubated at 37°C and 5% CO_2 for 72 hours in humidified trays to reduce edge effect. Following this incubation, paraformaldehyde (4% final concentration) in 1× phosphate buffered saline (PBS, Invitrogen, 10010023) was used to fix the cells for 1 hour. The cells were then subsequently treated with 5 µg/mL DAPI staining solution (Sigma Aldrich, D9542) for 1

hour. Next, the plates were imaged using an ImageXpress Micro automated high-content imager (Molecular Devices) using the 10× fluorescence objective. Images were analyzed automatically using a custom image analysis module (9, 11).

Software.

Chemical structures were prepared using ChemDraw Professional 18.1 (Perkin Elmer). EC_{50} and CC_{50} curves were generated using GraphPad Prism 8 (GraphPad Software).

Conflict of interest statement

The authors declare that they have no competing interests.

Acknowledgments

This work was supported by the Bill & Melinda Gates Foundation (OPP1107194). The screening experiments were performed at the UCSD Screening Core.

References

1. Lidani KCF, Andrade FA, Bavia L, Damasceno FS, Beltrame MH, Messias-Reason IJ, Sandri TL. 2019. Chagas disease: from discovery to a worldwide health problem. Front Public Health 7:166.
2. Prata A. 2001. Clinical and epidemiological aspects of Chagas disease. Lancet Infect Dis 1:92–100.
3. Caldas IS, Santos EG, Novaes RD. 2019. An evaluation of benznidazole as a Chagas disease therapeutic. Expert Opin Pharmacother 1–11.
4. Morillo CA, Marin-Neto JA, Avezum A, Sosa-Estani S, Rassi A, Rosas F, Villena E, Quiroz R, Bonilla R, Britto C, Guhl F, Velazquez E, Bonilla L, Meeks B, Rao-Melacini P, Pogue J, Mattos A, Lazdins J, Rassi A, Connolly SJ, Yusuf S, BENEFIT Investigators. 2015. Randomized trial of benznidazole for chronic chagas' cardiomyopathy. N Engl J Med 373:1295–1306.

5. Rassi A, Marin JA, Rassi A. 2017. Chronic Chagas cardiomyopathy: a review of the main pathogenic mechanisms and the efficacy of aetiological treatment following the BENznidazole Evaluation for Interrupting Trypanosomiasis (BENEFIT) trial. Mem Inst Oswaldo Cruz 112:224–235.
6. Pushpakom S, Iorio F, Eyers PA, Escott KJ, Hopper S, Wells A, Doig A, Guilliams T, Latimer J, McNamee C, Norris A, Sanseau P, Cavalla D, Pirmohamed M. 2019. Drug repurposing: progress, challenges and recommendations. Nat Rev Drug Discov 18:41–58.
7. Janes J, Young ME, Chen E, Rogers NH, Burgstaller-Muehlbacher S, Hughes LD, Love MS, Hull MV, Kuhen KL, Woods AK, Joseph SB, Petrassi HM, McNamara CW, Tremblay MS, Su AI, Schultz PG, Chatterjee AK. 2018. The ReFRAME library as a comprehensive drug repurposing library and its application to the treatment of cryptosporidiosis. Proc Natl Acad Sci USA 115:10750–10755.
8. Kim Y-J, Cubitt B, Chen E, Hull MV, Chatterjee AK, Cai Y, Kuhn JH, de la Torre JC. 2019. The ReFRAME library as a comprehensive drug repurposing library to identify mammarenavirus inhibitors. Antiviral Res 169:104558.
9. Moon S, Siqueira-Neto JL, Moraes CB, Yang G, Kang M, Freitas-Junior LH, Hansen MAE. 2014. An image-based algorithm for precise and accurate high throughput assessment of drug activity against the human parasite Trypanosoma cruzi. PLoS One 9:e87188.
10. Boudreau PD, Miller BW, McCall L-I, Almaliti J, Reher R, Hirata K, Le T, Siqueira-Neto JL, Hook V, Gerwick WH. 2019. Design of Gallinamide A Analogs as Potent Inhibitors of the Cysteine Proteases Human Cathepsin L and Trypanosoma cruzi Cruzain. J Med Chem.
11. Ekins S, de Siqueira-Neto JL, McCall L-I, Sarker M, Yadav M, Ponder EL, Kallel EA, Kellar D, Chen S, Arkin M, Bunin BA, McKerrow JH, Talcott C. 2015. Machine Learning Models and Pathway Genome Data Base for Trypanosoma cruzi Drug Discovery. PLoS Negl Trop Dis 9:e0003878.
12. Kraus JM, Verlinde CLMJ, Karimi M, Lepesheva GI, Gelb MH, Buckner FS. 2009. Rational modification of a candidate cancer drug for use against Chagas disease. J Med Chem 52:1639–1647.
13. Kraus JM, Tatipaka HB, McGuffin SA, Chennamaneni NK, Karimi M, Arif J, Verlinde CLMJ, Buckner FS, Gelb MH. 2010. Second generation analogues of the cancer drug clinical candidate tipifarnib for anti-Chagas disease drug discovery. J Med Chem 53:3887–3898.
14. Rodrígues-Poveda CA, González-Pacanowska D, Szajnman SH, Rodríguez JB. 2012. 2-alkylaminoethyl-1,1-bisphosphonic acids are potent inhibitors of the enzymatic activity of Trypanosoma cruzi squalene synthase. Antimicrob Agents Chemother 56:4483–4486.

15. Shang N, Li Q, Ko T-P, Chan H-C, Li J, Zheng Y, Huang C-H, Ren F, Chen C-C, Zhu Z, Galizzi M, Li Z-H, Rodrigues-Poveda CA, Gonzalez-Pacanowska D, Veiga-Santos P, de Carvalho TMU, de Souza W, Urbina JA, Wang AH-J, Docampo R, Li K, Liu Y-L, Oldfield E, Guo R-T. 2014. Squalene synthase as a target for Chagas disease therapeutics. PLoS Pathog 10:e1004114.
16. Bosc D, Mouray E, Cojean S, Franco CH, Loiseau PM, Freitas-Junior LH, Moraes CB, Grellier P, Dubois J. 2016. Highly improved antiparasitic activity after introduction of an N-benzylimidazole moiety on protein farnesyltransferase inhibitors. Eur J Med Chem 109:173–186.
17. Douc-Rasy S, Kayser A, Riou G. 1983. A specific inhibitor of type I DNA-topoisomerase of Trypanosoma cruzi: dimethyl-hydroxy-ellipticinium. Biochem Biophys Res Commun 117:1–5.
18. Kerschmann RL, Wolfson JS, McHugh GL, Dickersin GR, Hooper DC, Swartz MN. 1989. Novobiocin-induced ultrastructural changes and antagonism of DNA synthesis in Trypanosoma cruzi amastigotes growing in cell-free medium. J Protozool 36:14–20.
19. Gonzales-Perdomo M, de Castro SL, Meirelles MN, Goldenberg S. 1990. Trypanosoma cruzi proliferation and differentiation are blocked by topoisomerase II inhibitors. Antimicrob Agents Chemother 34:1707–1714.
20. Zuma AA, Cavalcanti DP, Maia MCP, de Souza W, Motta MCM. 2011. Effect of topoisomerase inhibitors and DNA-binding drugs on the cell proliferation and ultrastructure of Trypanosoma cruzi. Int J Antimicrob Agents 37:449–456.
21. Yu HA, Spira A, Horn L, Weiss J, West H, Giaccone G, Evans T, Kelly RJ, Desai B, Krivoshik A, Moran D, Poondru S, Jie F, Aoyama K, Keating A, Oxnard GR. 2017. A Phase I, Dose Escalation Study of Oral ASP8273 in Patients with Non-small Cell Lung Cancers with Epidermal Growth Factor Receptor Mutations. Clin Cancer Res 23:7467–7473.
22. Hirano T, Yasuda H, Hamamoto J, Nukaga S, Masuzawa K, Kawada I, Naoki K, Niimi T, Mimasu S, Sakagami H, Soejima K, Betsuyaku T. 2018. Pharmacological and Structural Characterizations of Naquotinib, a Novel Third-Generation EGFR Tyrosine Kinase Inhibitor, in EGFR-Mutated Non-Small Cell Lung Cancer. Mol Cancer Ther 17:740–750.
23. Tanaka H, Sakagami H, Kaneko N, Konagai S, Yamamoto H, Matsuya T, Yuri M, Yamanaka Y, Mori M, Takeuchi M, Koshio H, Hirano M, Kuromitsu S. 2019. Mutant-selective irreversible EGFR inhibitor, naquotinib, inhibits tumor growth in NSCLC models with EGFR activating mutations, T790M mutation and AXL overexpression. Mol Cancer Ther.
24. Klug DM, Tschiegg L, Díaz González R, Rojas-Barros DI, Perez-Moreno G, Ceballos-Perez G, García-Hernández R, Martínez-Martínez MS, Manzano P, Ruiz-Perez LM, Caffrey CR, Gamarro F, Gonzalez-Pacanowska D, Ferrins L, Navarro

M, Pollastri MP. 2019. Hit-to-lead optimization of benzoxazepinoindazoles as human African trypanosomiasis therapeutics. J Med Chem.

25. Simões-Silva MR, De Araújo JS, Peres RB, Da Silva PB, Batista MM, De Azevedo LD, Bastos MM, Bahia MT, Boechat N, Soeiro MNC. 2019. Repurposing strategies for Chagas disease therapy: the effect of imatinib and derivatives against Trypanosoma cruzi. Parasitology 146:1006–1012.
26. Wyllie S, Thomas M, Patterson S, Crouch S, De Rycker M, Lowe R, Gresham S, Urbaniak MD, Otto TD, Stojanovski L, Simeons FRC, Manthri S, MacLean LM, Zuccotto F, Homeyer N, Pflaumer H, Boesche M, Sastry L, Connolly P, Albrecht S, Berriman M, Drewes G, Gray DW, Ghidelli-Disse S, Dixon S, Fiandor JM, Wyatt PG, Ferguson MAJ, Fairlamb AH, Miles TJ, Read KD, Gilbert IH. 2018. Cyclin-dependent kinase 12 is a drug target for visceral leishmaniasis. Nature 560:192–197.
27. Diouf O, Carato P, Lesieur I, Rettori M, Caignard D. 1999. Synthesis and pharmacological evaluation of novel 4-(4-fluorobenzoyl)piperidine derivatives as mixed 5-HT1A/5-HT2A/D2 receptor ligands. Eur J Med Chem 34:69–73.
28. Spector T, Harrington JA, Porter DJ. 1991. Herpes and human ribonucleotide reductases. Inhibition by 2-acetylpyridine 5-[(2-chloroanilino)-thiocarbonyl]-thiocarbonohydrazone (348U87). Biochem Pharmacol 42:91–96.
29. Spector T, Lobe DC, Ellis MN, Blumenkopf TA, Szczech GM. 1992. Inactivators of herpes simplex virus ribonucleotide reductase: hematological profiles and in vivo potentiation of the antiviral activity of acyclovir. Antimicrob Agents Chemother 36:934–937.
30. Safrin S, Schacker T, Delehanty J, Hill E, Corey L. 1993. Potential for combined therapy with 348U87, a ribonucleotide reductase inhibitor, and acyclovir as treatment for acyclovir-resistant herpes simplex virus infection. J Med Virol Suppl 1:146–149.
31. Safrin S, Schacker T, Delehanty J, Hill E, Corey L. 1993. Topical treatment of infection with acyclovir-resistant mucocutaneous herpes simplex virus with the ribonucleotide reductase inhibitor 348U87 in combination with acyclovir. Antimicrob Agents Chemother 37:975–979.
32. Ellis S, Sexton DW, Steverding D. 2015. Trypanotoxic activity of thiosemicarbazone iron chelators. Exp Parasitol 150:7–12.

Figures

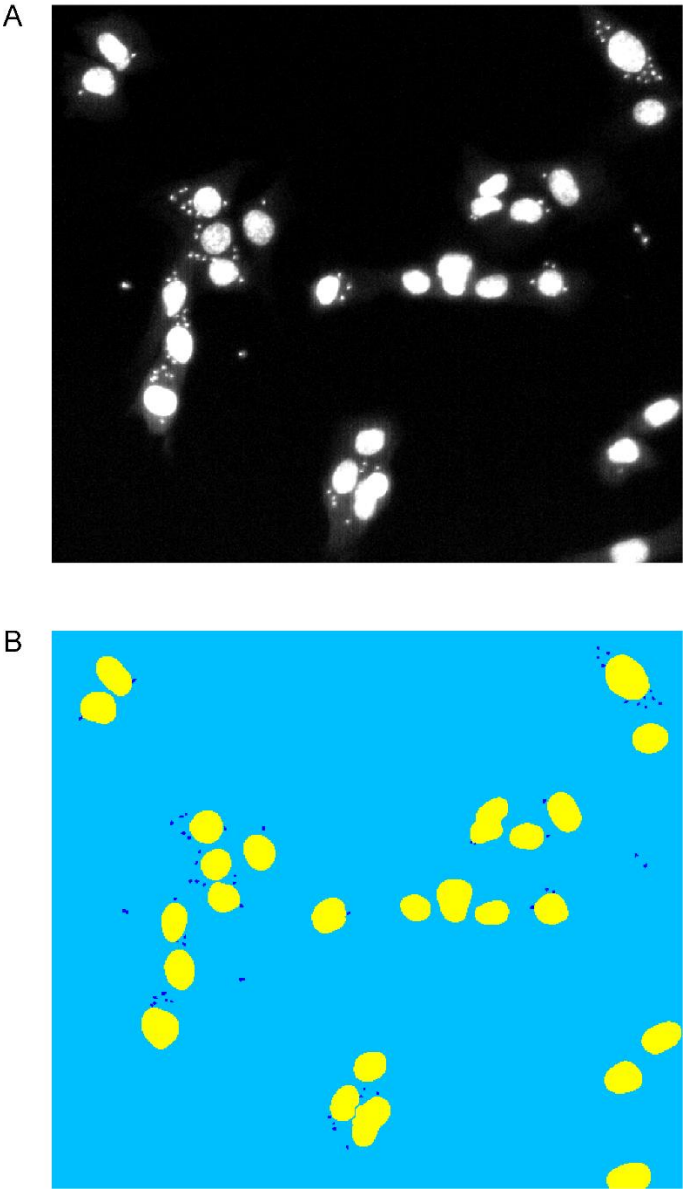

Figure 1. Automated segmentation analysis of *T. cruzi* amastigote and C2C12 mouse cardiomyocyte nuclei. A) Fluorescence microscopy image (10×magnification) of DAPI-stained C2C12 infected with CA-I/72 *T. cruzi* amastigotes 72 hours post-infection. B) Custom module segmentation of host and parasite cell nuclei using MetaXpress 5.0 (Molecular Devices). Host cell nuclei are in yellow and parasite nuclei are in dark blue.

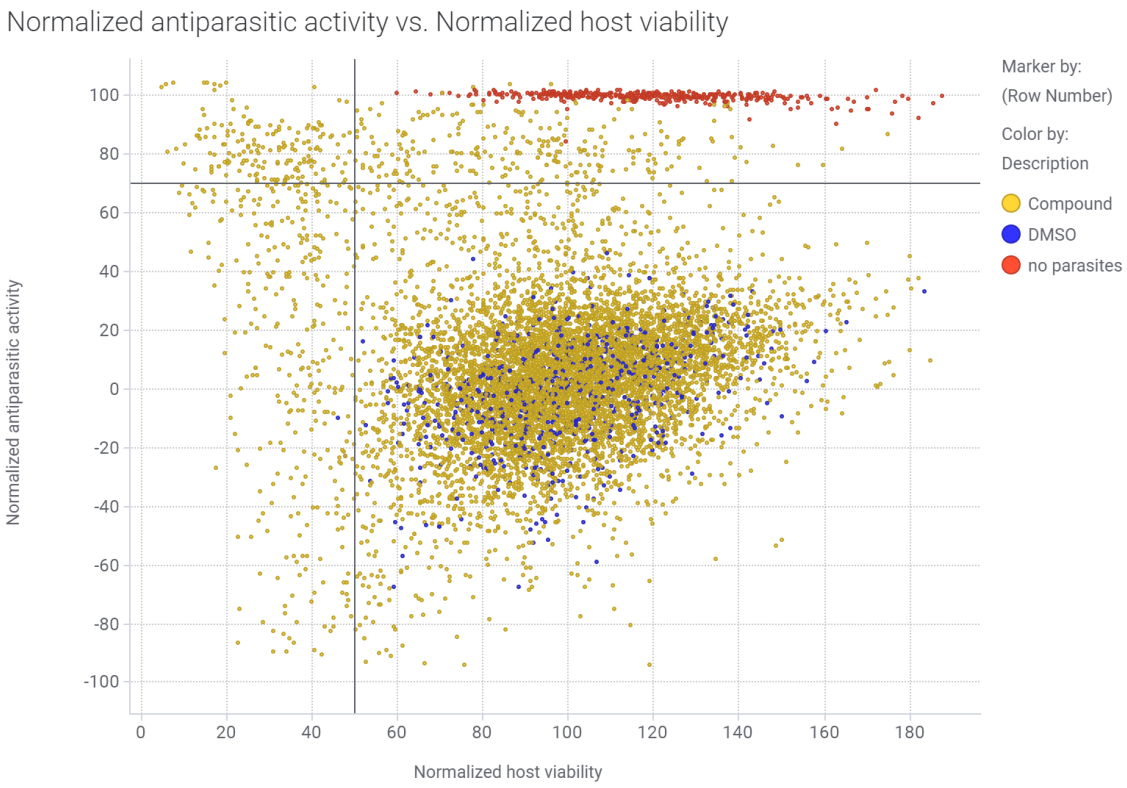

Figure 2. Primary screening data for the ReFRAME library against *T. cruzi* in the phenotypic high-content imaging assay. Scatter Plot of normalized % activity against CA-I/72 *T. cruzi* (Normalized antiparasitic activity %, Y-axis) and the host cell C2C12 viability % (Normalized host viability %, X-axis) for ReFRAME library. The red dots represent the uninfected controls, blue dots represent untreated controls (0.1% DMSO) and the yellow dots are the tested compounds. A vertical line at 50% Normalized host viability and a horizontal line at 70% Normalized antiparasitic activity highlights the top right quadrant where the compounds were selected as hits for dose-response confirmation.

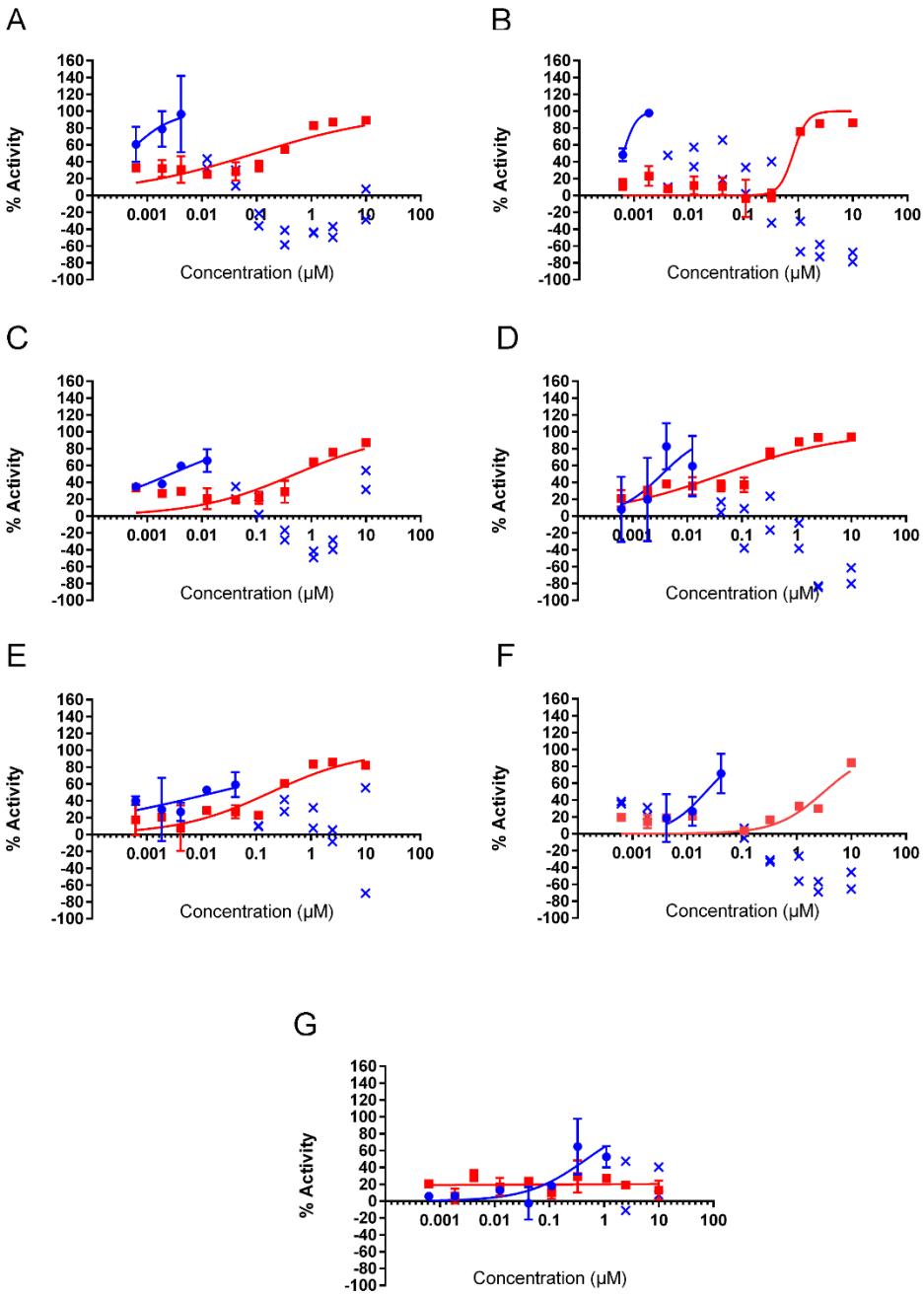

Figure 3. Dose response curves for validated hits from the ReFRAME library. % activity of the hit compounds NSC-706744 (A), 348U87 (B), ASP-8273 (C), XR 5944 (D), Prenyl-IN-1 (E), 3-[4-[4-(2-Methoxyphenyl)piperazine-1-yl]butyl]-6-[2-[4-(4-fluorobenzoyl)piperidine-1-yl]ethyl]benzothiazole-2(3H)-one (F) and Incadronate Disodium (G) against *T. cruzi* (blue curves, antiparasitic activity) and C2C12

cardiomyocytes (red curves, host cell toxicity) are shown for 2 replicate dose responses. Error bars indicate the standard error for each data point. Data values marked in blue with an “x” represent excluded antiparasitic activity data points (where host cell toxicity results in a drop-off of antiparasitic activity).

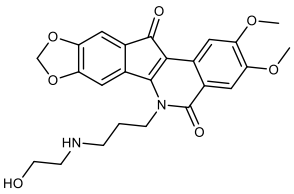

NSC-706744

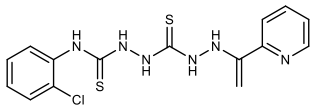

348U87

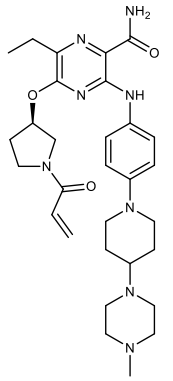

ASP-8273

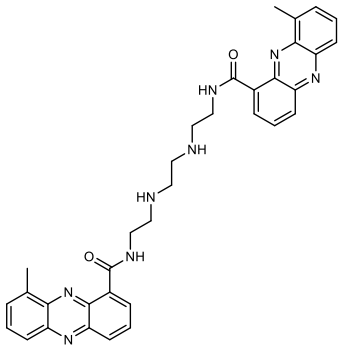

XR 5944

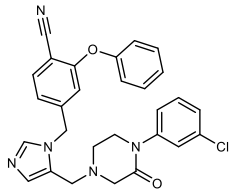

Prenyl-IN-1

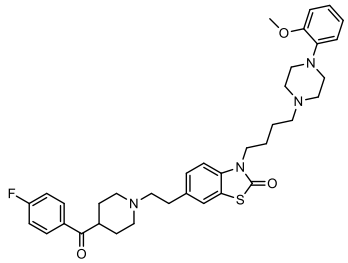

3-[4-[4-(2-Methoxyphenyl)piperazine-1-yl]butyl]-6-[2-[4-(4-fluorobenzoyl)piperidine-1-yl]ethyl]benzothiazole-2(3H)-one

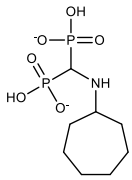

Incadronate

Figure 4. Chemical structures of hit compounds from the high-throughput screening campaign.

Tables

Table 1. EC_{50} and CC_{50} values for 7 validates hits from the ReFRAME library against CA-I/72 *T. cruzi* in the phenotypic high-content imaging assay ranked in order of potency. Values were calculated from duplicate dose response data, +/- standard error (SE). EC50 values are for *T. cruzi* CA-I/72 parasites. CC_{50} values are for C2C12 cardiomyocyte host cells. Selectivity index = CC_{50}/EC_{50}.

Compound Name	EC_{50} CA-I/72 *T. cruzi* (nM)	CC_{50} C2C12 (nM)	Selectivity Index (SI)
NSC-706744	0.44 +/- 0.08	94 +/- 56	214
348U87	0.63 +/- 0.45	815 +/- 215	1294
ASP-8273	2.7 +/- 1.9	515 +/- 280	191
XR 5944	3.5 +/- 6.8	46 +/- 21	13
Prenyl-IN-1	18 +/- 12	182 +/- 90	10

3-[4-[4-(2-Methoxyphenyl)piperazine-1-yl]butyl]-6-[2-[4-(4-fluorobenzoyl)piperidine-1-yl]ethyl]benzothiazole-2(3H)-one	22 +/- 23	3,190 +/- 1,202	145
Incadronate Disodium	480 +/- 385	> 10,000	> 20